New antidiabetic targets of α-glucosidase inhibitory peptides, SVPA, SEPA, STYV and STY: Inhibitory effects on dipeptidyl peptidase-IV and lipid accumulation in 3T3-L1 differentiated adipocytes with scavenging activities against methylglyoxal and reactive oxygen species

Mohammed Auwal Ibrahim[1,3*], June C. Serem[2], Megan J. Bester[2], Albert W. Neitz[1] and Anabella R.M. Gaspar[1]

[a]*Department of Biochemistry, Genetics and Microbiology, University of Pretoria, Pretoria 0002, South Africa*
[b]*Department of Anatomy, University of Pretoria, Pretoria 0002, South Africa*
[c]*Department of Biochemistry, Ahmadu Bello University, Zaria, Nigeria*

***Correspondence to:** Dr. Mohammed Auwal Ibrahim, Department of Biochemistry, Genetics and Microbiology, Faculty of Natural and Agricultural Sciences, University of Pretoria, Pretoria 0002, South Africa E mail: mauwalibrahim@gmail.com or maibrahim@abu.edu.ng

Abstract

Type 2 diabetes mellitus (T2DM) is a multifactorial disease that requires multiple therapeutic strategies for its management. Bioactive peptides with multiple anti-diabetic targets are attractive therapeutic molecules The present study was conducted to identify additional anti-diabetic targets of α-glucosidase inhibitory peptides, SVPA, SEPA, STYV, STY. The α-glucosidase inhibitory activity of the peptides was in the order STYV > STY > SEPA > SVPA while molecular docking against human dipeptidyl peptidase IV (DPP-IV) showed that SVPA had the best binding affinity. In contrast, *in vitro* studies indicated that SEPA had a significantly higher (P<0.05) DPP-IV inhibitory activity (IC_{50} = 5.78 ± 0.19 mM) than other peptides. SVPA and SEPA showed mixed inhibition pattern while STYV and STY were uncompetitive inhibitors of the enzyme. IPI (diprotin A), STYV and STY were not cytotoxic while SEPA displayed some cytotoxicity. In differentiated 3T3-L1 adipocytes, SVPA and STYV were found to induce a significant (P<0.05) decrease in intracytoplasmic lipid accumulation when added during the differentiation process while STY, GSH and IPI caused significant reduction (P<0.05) in the lipid accumulation when added after the differentiation. The SVPA, SEPA and STYV were better scavengers of methylglyoxal than STY but STYV had the best scavenging activities toward reactive oxygen species and nitric oxide. It was concluded that the four α-glucosidase inhibitory peptides including IPI have multiple targets against type T2DM but, overall, of the four peptides evaluated, STYV tends to have better potential for application as multifunctional anti-diabetic peptide.

Key words: Type 2 diabetes mellitus; multifunctional peptides; DPP-IV inhibition; α-glucosidase inhibitory peptides; methylglyoxal; antioxidant activity

Introduction

Bioactive peptides are specific peptide fragments with 2-20 amino acid residues that have attracted significant interest in the food and health sectors (Udenigwe 2014). This is due to the multiple bioactivities of these peptides that can beneficially influence human health. These include antimicrobial (Wang et al. 2016), antioxidant (Byun et al. 2009), antihypertensive (Lafarga et al. 2014), anti-inflammatory (Korhonen and Pihlanto 2007), anticancer (Yin et al. 2013), antithrombotic (Park and Nam 2015) and antidiabetic (Mojica and de Majia 2016; Zhang et al. 2016) activities. Furthermore, these peptides have favourable pharmacokinetic profiles, good solubility properties, low toxicity and immunogenicity and in addition, ease of modification to improve stability and binding affinity (Wu et al. 2017). With the rapid development in next generation sequencing, bioinformatics and research in food technology, many bioactive peptides are being discovered using different experimental strategies (Li et al. 2018; Ibrahim et al. 2018a). This is evident by the high number of *in silico* databases and bioinformatics tools (Agyei et al. 2018) with new ones continuously being developed (Li et al. 2018). Indeed, some bioactive peptides have been approved by the FDA for commercialization as therapeutic molecules and these are listed in the therapeutic peptides database (http://crdd.osdd.net/ragha va/thpdb/) (Usmani et al. 2017). The search for novel bioactive peptides, especially with multifunctionality, is an important area scientific endeavour because of their unique pharmaceutical potentials.

An important public health problem where bioactive peptides are showing promising therapeutic potentials is diabetes mellitus which is a chronic metabolic disorder that affects 8.5% of the global population in 2014 with a projected rise to 10.1% by 2035 (Guariguata et al. 2014). Among the different types of diabetes mellitus, type 2 diabetes (T2DM) is the most prevalent accounting for > 90% of the diabetic populations. A prominent characteristic of T2DM is high blood glucose levels as a result of deficiency in insulin secretion and/or action which consequently affects carbohydrate, lipid and protein metabolism in addition to the induction of macro-and microvascular complications (De Fronzo et al. 2014). In fact, T2DM is considered to be a multifactorial disease that requires multiple therapeutic strategies for its management (De Fronzo et al. 2014). Consequently, several classes of drugs have been developed that target different aspects of the T2DM pathogenesis. These drugs include sulfonylureas, biguanides,

thiazolidinediones, sodium-glucose cotransporter 2 inhibitors, gliptins, α-glucosidase inhibitors among others, however, each of these classes of drugs has side effects (Inzucchi et al. 2015). In a previous study involving a total of 43 fully sequenced α-glucosidase inhibitory peptides, STYV was identified as the most potent peptide (Ibrahim et al. 2018a). However, *in silico* simulated gastrointestinal digestion revealed that STYV was unstable while molecular docking studies suggested that STY (digestion fragment of STYV) might have better α-glucosidase inhibitory potentials than STYV (Ibrahim et al. 2018a). Subsequently, we used a rational drug design approach to design two novel and gastrointestinally stable α-glucosidase inhibitory peptides, SVPA and SEPA which were evaluated *in vitro* (Ibrahim et al. 2018b). However, peptides with more than one antidiabetic target are preferred than peptides with only one specific target. These multifunctional peptides can simultaneously trigger, modulate or inhibit multiple pathways. Hence, the development of a peptide or any agent that target multiple processes associated with diabetes such as specific enzyme targeting, reduction of the levels of toxic metabolites such as methylglyoxal (MG) and reactive oxygen species (ROS) that form as a result of a disrupted glucose homeostasis are promising and attractive molecules for the food and pharmaceutical industries.

Dipeptidyl peptidase-IV (DPP-IV; EC 3.4.14.5) is a serine protease that rapidly inactivates incretin hormones and thereby reducing pancreatic glucose-dependent insulin secretion, and consequently plays a pivotal role in glucose homoestasis (Lacroix and Chan 2016). Currently, DPP-IV inhibitors such as sitagliptin and vildagliptin are clinically available for T2DM treatment because they prolong the action of incretin hormones and promote glucose-dependent insulin secretions (Mulvihill 2018). In addition to lowering blood glucose levels, it is also important to lower the lipid levels in T2DM (Mulvihill 2018; Cao et al. 2018). This is because alteration of lipid metabolism and fat accumulation are important etiological factors in the development of diabetes-associated macrovascular complications (Mulvihill 2018; Cao et al. 2018). In this process, adipocytes play a pivotal role. The 3T3-L1 cell line is a well-established cell line that can easily differentiate into adipocytes in the presence of specific factors and allow laboratory based screening of the effects of drugs including peptides on lipid metabolism and accumulation in addition to selective adipocyte cytotoxicity studies (Semaan et al. 2018). These studies are important considering the emerging role of adipocytes as an important drug target for

T2DM and obesity-mediated metabolic syndrome because these cells express high amounts of glucose transporter-4 (GLUT 4) and peroxisome proliferator-activated receptor-γ (PPAR- γ) (Hasan et al. 2017). A consequence of a disrupted glucose homeostasis is MG accumulation (Hadi and Suwaidi, 2007). Under normal metabolic conditions, MG is metabolized to lactate by glyoxylase but in the diabetic condition, glyoxalase activity is reduced leading to MG accumulation which in turn promotes the formation of advanced glycosylated end products (AGEs) (Vulesevic et al. 2016). Moreover, the formation of AGEs is a vital mechanism of pathogenesis associated with the induction of oxidative stress and diabetic complications (Giacco and Brownlee 2010). Increased oxidative stress as a result of ROS and reactive nitrogen species (formed from the reaction of nitric oxide (NO) and superoxides) is considered as a single unifying mechanism that plays pivotal role in all aspects of T2DM pathogenesis and the associated complications (Giacco and Brownlee 2010). Therefore, the development of a multifunctional agent that modulate the activity of enzymes associated with glucose homeostasis, scavenge the MG, ROS and NO radicals would ultimately be beneficial to patients with T2DM.

In order to increase the therapeutic and pharmaceutical relevance of the previously identified α-glucosidase inhibitory peptides, SVPA, SEPA, STYV and STY; the present study was designed to further investigate the effects of the peptides on DPP-IV inhibition using *in silico* and *in vitro* models. In addition, the effects of these peptides on lipid accumulation in 3T3-L1 differentiated adipocytes and the ability to scavenge MG, ROS and NO radicals were also investigated.

Materials and methods

Chemicals and reagents

Yeast α-glucosidase, kidney DPP-IV, p-nitrophenyl-α-D-glucopyranoside (pNPG), Gly-Pro-p-nitroanilide (GPpNA), diprotin A, insulin, dexamethasone, Dulbecco's modified Eagle's medium (DMEM), rosiglitazone, isobutylmethylxanthine (IBMX), Oil Red O, antibiotic solution (10000 units penicillin, 10 mg streptomycin, 25 μg amphotericin B per mL), bovine serum albumin (BSA), methylglyoxal (MG), reduced glutathione (GSH), 2,2'-azobis(2-amidinopropane) dihydrochloride (AAPH) and fluorescein were obtained from Sigma-Aldrich Chemical Company (Johannesburg, South Africa). Sulphanilamide, sodium nitroprusside, dimethylsulfoxide

(DMSO), 3-[4,5-dimethylthiazol-2-yl]-2,5-diphenyltetrazolium bromide (MTT) and N-(1-naphthyl)-ethylenediamine-dihydrochloride (NED) were procured from Merck (Johannesburg, South Africa) while foetal calf serum (FCS) was obtained from Capricon Scientific (GmBH, Germany). The peptides, SVPA, SEPA, STYV and STY were obtained from Genscript (New Jersey, USA).

Molecular docking analysis

In order to determine the binding potentials of the four peptides toward human DPP-IV, the peptides were initially subjected to molecular docking analysis. The 3D crystal structures of the human DPP-IV complexed with diprotin A (PDB ID 1WCY resolved to 2.20Å by x-ray diffraction) was retrieved in PDB format from the protein data bank (www.rcsb.org) and UCSF chimera version 1.11.2 (www.cgl.ucsf.edu/chimera/) (Pettersen et al. 2004) was used to remove the diprotin A and other co-crystallized molecules from the protein structure. Subsequently, the dock prep tool of the chimera software (Pettersen et al. 2004) was used to prepare the protein and the peptide ligands for the molecular docking. All default parameters for the dock prep tool in chimera were used and the structures were retrieved as PDB formats after the dock prep. Thereafter, the PDB prepared versions of the protein and the peptide ligands were opened in chimera and subjected to the Autodock Vina tool (Trott and Olson 2010) in the same software. The grid sizes (xyz points) were set as 53.7338, 47.5117 and 156.0177 while the grid centers were designated at dimensions (x, y and z) 49.3051, 60.8384 and 51.5917. Other parameters of Autodock Vina in chimera were left as default. AutoDock Vina employs iterated local search global optimizer and all output files were saved in pdbqt format. After the successful docking in Vina, the minimum binding free energy for each of the peptides was recorded while the docking pose was extracted and aligned with the receptor structure for further analysis of hydrogen bond interactions.

Peptide synthesis and preparation

The peptides, SVPA, SEPA, STYV and STY, were synthesized using Flexpeptide^{TM} technology by GenScript. The purity and molecular mass of the peptides were determined by the manufacturer using reverse phase high performance liquid chromatography and mass spectrometry, respectively. Amino acid analysis of the peptides was also performed by the

vendor and was used for the peptide quantification. Stock peptide solutions were prepared in sterile deionized double distilled water.

α-Glucosidase inhibitory activity of the peptides

Initially, it was important to validate the previously reported α-glucosidase inhibitory activity (IC_{50} value) of STYV (Singh and Kaur 2015; Ibrahim et al. 2018a) and STY (not earlier reported) against α-glucosidase in our laboratory. The inhibitory activity of the peptides was assayed according to a previously described method (Ibrahim et al. 2014) with slight modifications. Briefly, 50 µL of each peptide at a final concentration of 62.5-500 µM was incubated with 25 µL of 0.5 U/mL α-glucosidase solution in 100 mM phosphate buffer (pH 6.8) at 37 ^{o}C for 60 min. Thereafter, 25 µL of a 5 mM pNPG solution in 100 mM phosphate buffer (pH 6.8) was added and the mixture was further incubated at 37 ^{o}C for 30 min. The absorbance of the released *p*-nitrophenol was measured at 405 nm using Spectramax paradigm multi-mode microplate reader (Molecular Devices LLC, USA) and the inhibitory activity was expressed as percentage of a control sample without the inhibitors. The α-glucosidase inhibitory activity of the peptides was calculated by using the following formula:

$$\alpha - \text{Glucosidase inhibitory activity } (\%) = \left(1 - \frac{\text{As}}{\text{Ac}}\right) \text{x } 100$$

where As and Ac are absorbance of sample and absorbance of control, respectively. The concentrations of the peptides resulting in 50% inhibition of enzyme activity (IC_{50} values) were determined using the straight-line equations of the percentage inhibitory activity against the respective logarithm of peptide concentrations (Shai et al. 2010).

DPP-IV inhibitory activity of the peptides

The DPP-IV inhibitory activity of the four peptides was determined using the method described by Konrad et al. (2014). Briefly, 50 µL of the peptides at final concentrations of 62.5-500 µM was incubated with 25 µL 0.02 U/mL DPP-IV re-suspended in 100 mM Tris-HCl buffer (pH 8.0) at 37 ^{o}C for 60 min. Thereafter, 25 µL of 6 mM GPpNA was added to the reaction mixture and further incubated at 37 ^{o}C for 60 min. The absorbance of the released *p*-nitroanilide was measured at 405 nm using Spectramax paradigm multi-mode microplate reader (Molecular

Devices LLC, USA) and the inhibitory activity was expressed as percentage of a control sample without the inhibitors. A standard DPP-IV inhibitor, diprotin A (IPI), served as a positive control. The DPP-IV inhibitory activity of the peptides was calculated by using the following formula:

$$\text{DPP} - \text{IV inhibitory activity (\%)} = \left(1 - \frac{\text{As}}{\text{Ac}}\right) \text{x } 100$$

where As and Ac are absorbance of sample and absorbance of control respectively. The concentrations of the peptides resulting in 50% inhibition of enzyme activity (IC_{50} values) were determined using the straight-line equations of the percentage inhibitory activity against the respective logarithm of peptide concentrations (Shai et al. 2010).

Mechanism of DPP-IV inhibition

The peptides were subjected to enzyme inhibition kinetic experiments to determine the type of inhibition exerted on DPP-IV under *in vitro* conditions. The experiment was conducted according to the protocol described above at two fixed final concentrations of the peptides (250 and 500 µM) with a variable concentration of GPpNA (0.75 – 6 mM). The data obtained were used to construct Lineweaver-Burk plots to determine the type of inhibition of the peptides against the DPP-IV.

Growth and maintenance of cell cultures

3T3-L1 cells were obtained at passage 40 from CELLONEX separations and used between passage 43 - 48. Cells were maintained in DMEM supplemented with 10% (v/v) foetal bovine serum and 1% (v/v) antibiotics at 37 °C in an atmosphere of 5% CO_2 and 90% humidity until confluence, with splitting at 3-4 days intervals.

Cytotoxicity of 3T3-L1 cells (pre-adipocytes and adipocytes)

Undifferentiated/pre-adipocyte 3T3-L1 cells were seeded at a concentration of $0.4X10^4$ per 90 µL in a 96 well plate and left to attach overnight at 37˚C, 5% CO_2.

For the differentiation of the 3T3-L1 cells, the pre-adipoctye cells were seeded at a concentration of 0.1 x 10^4 per 100 µL in a 96 well plate and grown to confluence for three days. On day 4, the cells were then induced to differentiate using 100 µL differentiation medium 1

(DM1, DMEM supplemented with final concentrations of 10 µg/mL insulin, 25 mM IBMX, 50 µM dexamethasone and 100 µM rosiglitazone). DM1 was replenished twice for every 6 days. On day 10, DM1 was replaced with DM2 (DMEM with only 10 µg/mL insulin) for 3 days. On day 14, the medium was replaced with DMEM only. Both undifferentiated and differentiated cells were tested for cytotoxicity by exposing them to 10 µL peptide (50 and 100 µM, final concentration) for 24 h at 37˚C, 5% CO_2. Cytotoxicity was then determined using the MTT assay.

MTT assay

The potential cytotoxicity of the peptides towards both differentiated and undifferentiated 3T3-L1 cells was determined using the MTT assay. Following incubation with peptides, 10 µL of 1 mg/mL MTT (91 µg/mL, final concentration) solution was added to each well and incubated for 3 h at 37 °C and 5% CO_2. After incubation, the medium containing MTT was removed and the plate left to dry at room temperature. The purple formazan crystals were dissolved with 50 µL 25% (v/v) DMSO in ethanol with shaking for approximately 5 min. The absorbance of the solution in each well was measured at 570 nm using a BioTek plate reader. Cell viability in the presence of peptides was expressed as a percentage relative to the control containing (undifferentiated or differentiated as appropriate) cells only (100% cell viability).

Prevention of lipid-accumulation in adipocyte 3T3-L1 cells

Peptides were tested for their anti-lipid formation using differentiated 3T3-L1 cells using two strategies; (i) Cells were differentiated for 14 days as described above and were then exposed to peptide (50 and 100 µM, final concentration) for 24 h (ii) With each addition of differentiation medium, peptides (50 and 100 µM, final concentration) were added concurrently (days 4, 7 and 10) until day 14. For both experiments, lipid accumulation was then determined with Oil red O staining.

Oil Red O staining

Oil Red O staining was used to detect oil droplets in adipocytes. The cells were fixed with 2% (v/v) formaldehyde for 30 min at 37˚C, 5% CO_2. Thereafter, the formaldehyde was discarded and the plates were air dried. The Oil Red O solution (three parts of 0.5% Oil-Red O (w/v) in

60% isopropyl alcohol and two parts water) was the added for 30 min. After staining of the lipid droplets, the Oil Red O staining solution was removed and the plates were rinsed with water and dried. Images of the stained lipid droplets were collected on an Olympus microscope (Olympus, Tokyo, Japan). Subsequently, the dye was extracted from the stained cells with 60% isopropanol and quantified by measuring the absorbance at 405 nm. The percentage lipid accumulation was calculated compared to the unexposed differentiated adipocytes as 100% lipid formation.

MG scavenging activity of the peptides

The method described of Siddiqui et al. (2016) was used, with slight modifications, to investigate the ability of the peptides to scavenge MG. A volume of 25 µL of each peptide (31.25 – 250 µM) was transferred into a 96-well fluorescence plate followed by the addition of 25 µL MG (56 mM initial concentration). Thereafter, 50 µL of 100 mM phosphate buffer (pH 7.4) was added to a final volume of 100 µL in each well. The plate was then incubated at 37˚C for 7 days under a sterile 5% CO_2 environment. The positive control contained BSA (40 mg/mL initial concentration), MG and phosphate buffer, the negative control consisted of MG and phosphate buffer only and the experimental blank consisted of the peptides in buffer. After incubation, the florescence was measured at 330nm (excitation) and 420 nm (emission) wavelengths using a FLUOstar OPTIMA plate reader (BMG Labtechnologies, Offenburg, Germany). The amount of AGEs formed was expressed as percentage of florescence in the presence of the peptides and MG relative to the positive control set up containing MG and BSA (100% AGEs formation).

Oxygen radical absorbance capacity (ORAC) antioxidant assay

This assay was performed according to the method of Ou et al. (2002). Briefly, 165 µL of fluorescein (0.139 nM) was added to each well of a 96 - well plate followed by 10 µL of each peptide sample (5-50 µM final concentration) added to the wells containing fluorescein. GSH was included as a peptide, positive control. Thereafter, 25 µL of 0.24 mM AAPH was added and fluorescence was immediately measured every 60 seconds for 120 minutes, to generate 120 cycles, at an excitation and emission wavelength of 485 nm and 520 nm, respectively using a FLUOstar OPTIMA plate reader (BMG Labtechnologies, Offenburg, Germany). Trolox was used at final concentrations of 0 – 50 µM. The positive control contained fluorescein with AAPH

only whereas the vehicle control contained fluorescein with ddH_2O. The area under curve was calculated and the antioxidant activity of each sample was expressed as μM TE.

NO Scavenging activity of the peptides

A quantitative chemical assay with Griess reagent was used (Giustarini et al. 2008) with slight modifications to determine the ability of the peptides including GSH (positive control) to directly scavenge NO. The reaction involved the addition of 40 μL of 5 mM sodium nitroprusside (SNP) solution dissolved in 0.1 M phosphate buffered saline (pH 7.4) and left to stand for 1 h in the light) to 10 μL of each of the peptide at a final concentration of 12.5 - 100 μM, followed by incubation for 1 h at 37 ^{o}C. GSH and IPI were used as controls. Thereafter, 50 μL of Griess reagent (1 % sulfanilamide and 0.1% NED in 2.5% phosphoric acid) was added. The absorbance was measured using a BioTek plate reader at 570 nm. The amount NO scavenged in the presence of peptides was expressed as a percentage relative to the control containing all reagents except peptide (100% NO).

Statistical analysis

Values are presented as mean ± SD of two independent experiments done in triplicates and the data were analyzed by using a statistical software package (SPSS for Windows, version 18, IBM Corporation, NY, USA) using Tukey's-HSD multiple range *post-hoc* test. Values were considered significantly different at $P < 0.05$.

Results

Prior to investigating the *in vitro* DPP-IV inhibitory activity of the four peptides, it was necessary to determine the *in silico* binding potential toward the enzyme. SVPA had the best DPP-IV binding affinity of all the peptides (Table 1). However, SVPA did not form any hydrogen bond interaction with the enzyme while SEPA had 6 hydrogen bond interactions (Fig. 1) followed by STYV and STY with 3 hydrogen bonds each (Table 1). The distance of the hydrogen bonds was within the range of 1.988 to 3.618 Å. With respect to binding at the active site pocket, STYV had a more precise docking pose at the active site (Fig. 1) which was followed by STY. Indeed, all the 3 hydrogen bond interactions between STYV and the enzyme

were mediated with active site residues (Y662 and Y547) while none of the hydrogen bond interactions between STY or SEPA and the enzyme involved any active site residue (Table 1).

Table 1 Binding free energy (kcal/mol) and other docking results of SVPA, SEPA, STYV and STY with the human DPP-IV

Peptide ligand	Binding energy (kcal/mol)	Number of hydrogen bonds	Interacting residue of peptide	Interacting residue of DPP-IV	Hydrogen bond distance (Å)
SVPA	-8.4	0	-	-	-
SEPA	-7.9	6	E2	R356	2.093
			P3	R358	2.330
			A4	R358	2.406
			A4	R358	2.436
			P3	D302	3.093
			P3	P359	3.618
STYV	-7.6	3	S1	Y662	2.064
			T2	Y547	2.004
			S1	Y662	2.104
STY	-6.7	3	S1	F357	1.988
			Y3	R669	2.023
			Y3	R669	2.291

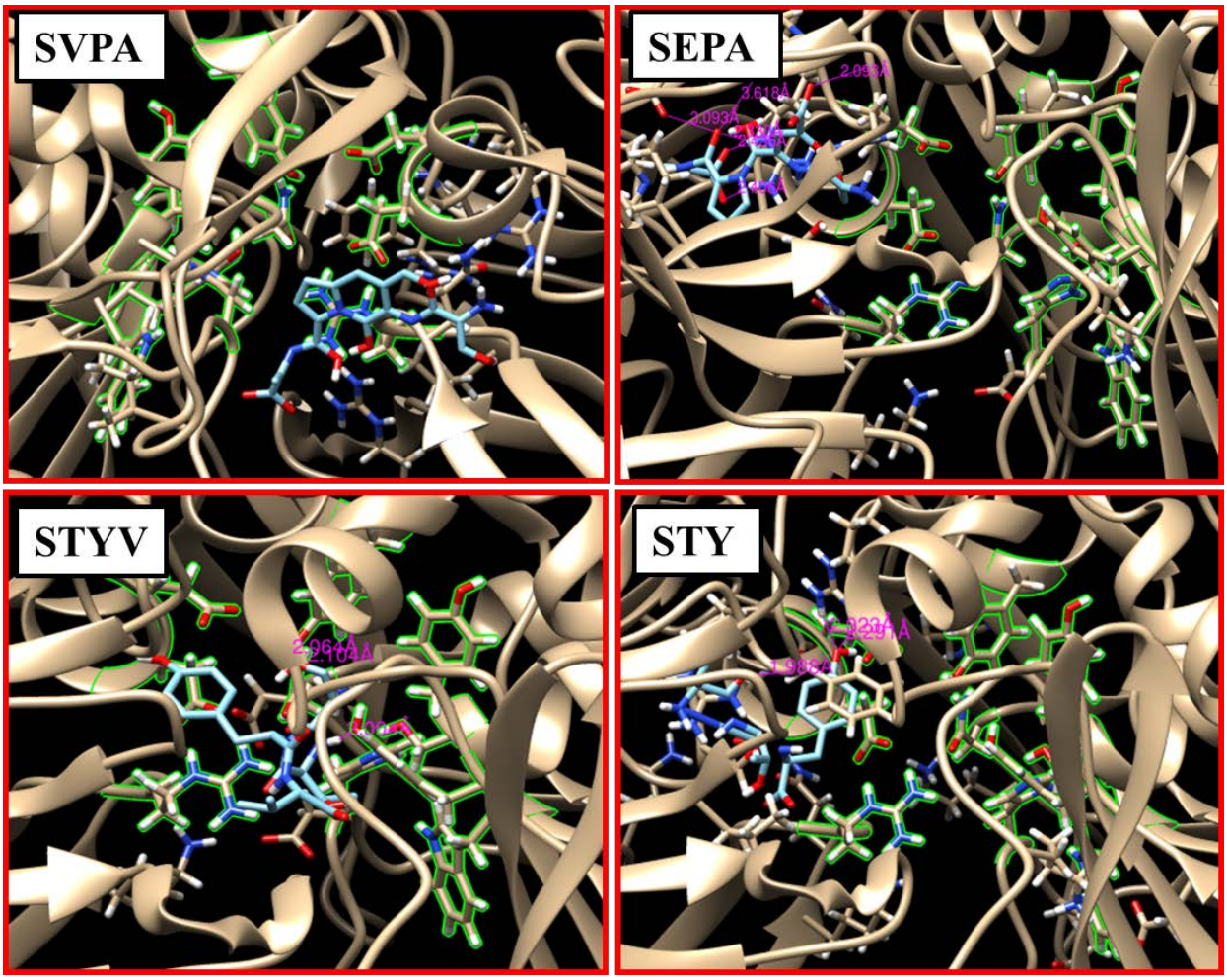

Fig. 1 The molecular docking pose of SVPA, SEPA, STYV and STY on the human DPP-IV. The pink lines represent the hydrogen bonds with the respective bond distances while the green area indicated the active site residues. The binding site has been zoomed out for each peptide-DPP-IV interaction

After establishing the *in silico* binding potential of the peptides toward DPP-IV, the *in vitro* α-glucosidase inhibitory activities of STYV and STY were initially investigated for validation and comparative purposes where it was found out that STYV had the most potent α-glucosidase inhibitory activity (Table 2), although the IC_{50} value was not significantly (P> 0.05) different with that of STY. Subsequently, the inhibition of DPP-IV was determined and it was observed that SEPA was the most potent DPP-IV inhibitor among the peptides with the exception of the positive control, diprotin A (Table 2). Overall, the α-glucosidase inhibitory activity of the peptides was in the order STYV > STY > SEPA > SVPA while the DPP-IV inhibitory activity was in the order SEPA > SVPA > STYV > STY (Table 2). Enzyme kinetic

analysis of the peptides against the DPP-IV revealed that SVPA and SEPA were mixed inhibitors of the enzyme while STYV and STY were uncompetitive inhibitors (Fig. 2).

Table 2 IC_{50} values for α-glucosidase and DPP-IV inhibitions by SVPA, SEPA, STYV and STY

Peptide/standard	IC_{50} (mM)	
	Validated α-glucosidase inhibition	DPP-IV inhibition
SVPA	4.56 ± 1.56^{c} (Ibrahim et al. 2018)	31.74 ± 1.09^{c}
SEPA	0.79 ± 0.16^{b} (Ibrahim et al. 2018)	5.78 ± 0.19^{b}
STYV	0.35 ± 0.09^{a}	162.96 ± 7.89^{d}
STY	0.46 ± 0.03^{a}	284.22 ± 3.50^{e}
IPI (diprotin A)	-	0.0035 ± 0.001^{a}

Data are expressed as mean ± SD of two independent experimentss done in triplicates. $^{a\text{-}e}$Values with different subscript letters along a column are significantly different from each other (Tukey's-HSD multiple range post hoc test, $P < 0.05$)

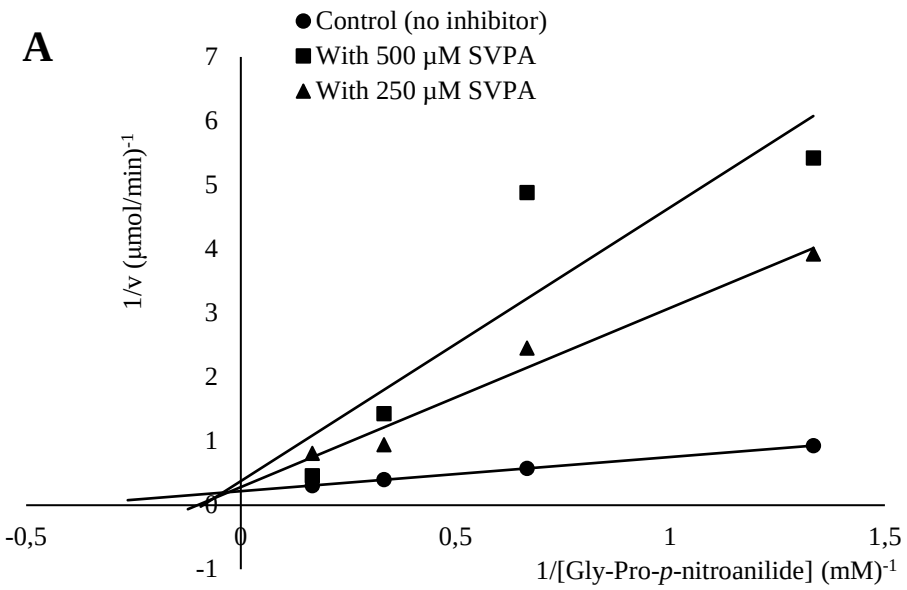
A
Control (no inhibitor)
With 500 µM SVPA
With 250 µM SVPA
1/v (µmol/min)-1
7
6
5
4
3
2
1
0
-1
-0,5
0
0,5
1
1,5
1/[Gly-Pro-p-nitroanilide] (mM)-1

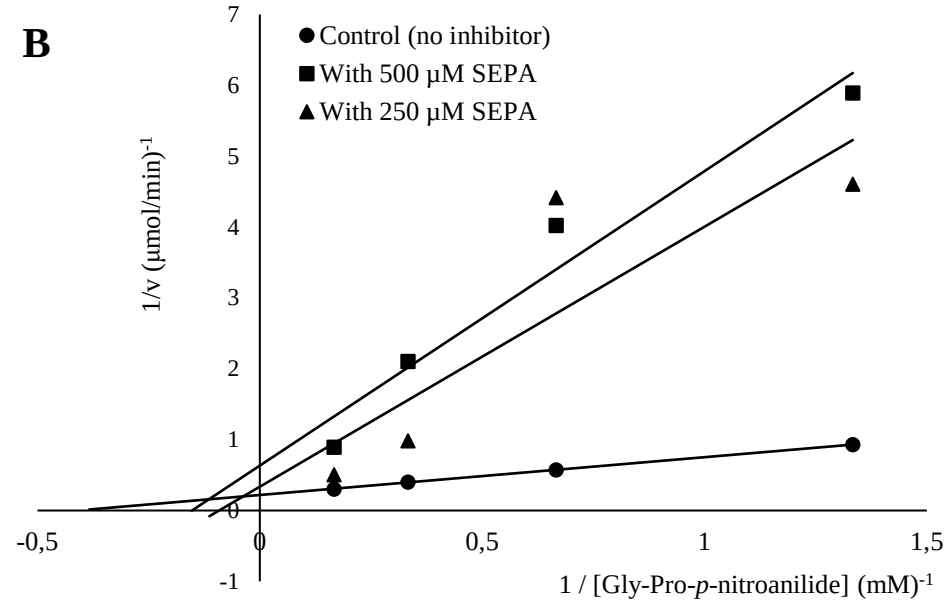
B
Control (no inhibitor)
With 500 µM SEPA
With 250 µM SEPA
1/v (µmol/min)-1
7
6
5
4
3
2
1
0
-1
-0,5
0
0,5
1
1,5
1 / [Gly-Pro-p-nitroanilide] (mM)-1

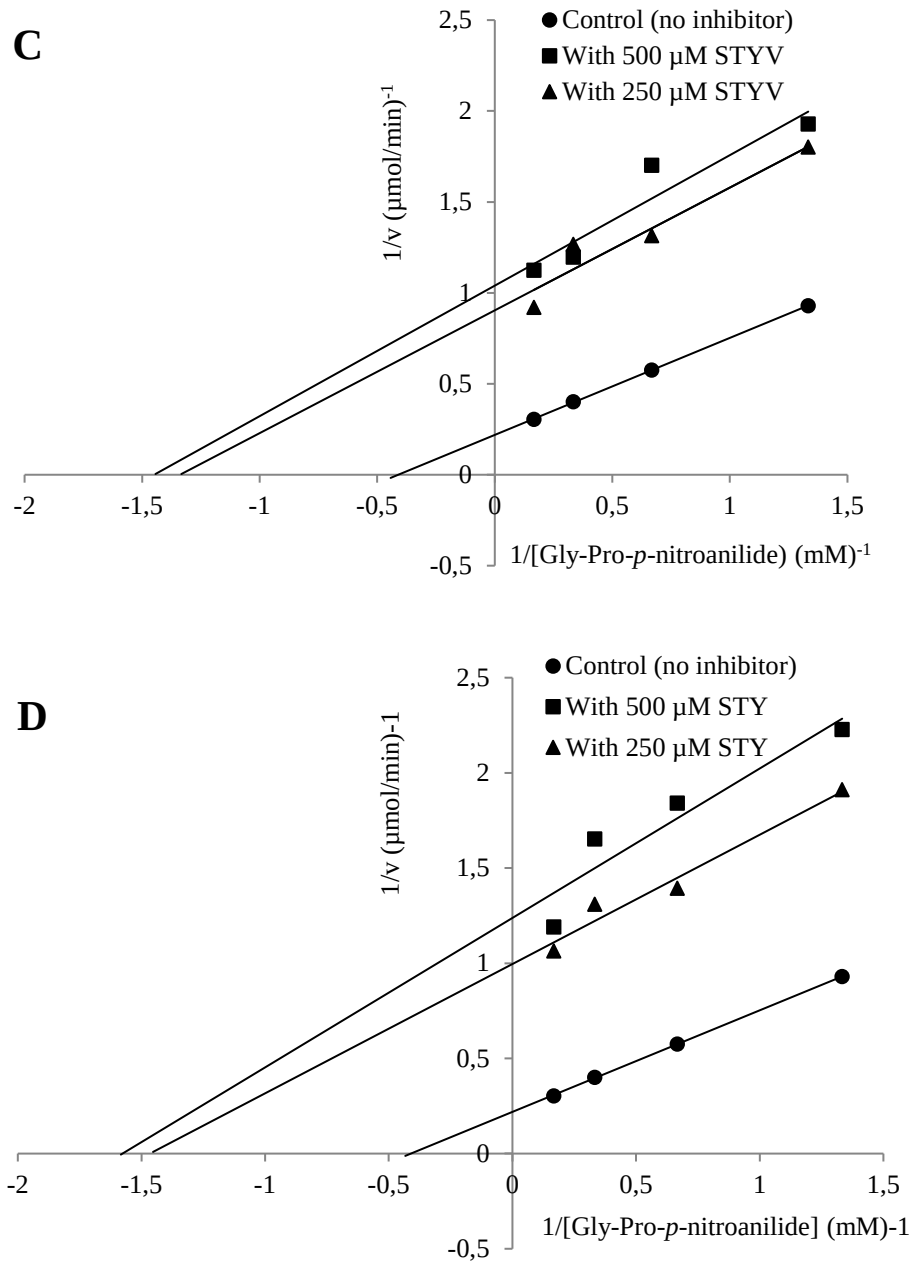

Fig. 2 Inhibition kinetics of SVPA (**A**), SEPA (**B**), STYV (**C**) and STY (**D**) against DPP-IV using Lineweaver-Burke's analysis. Each data point represents a mean of two independent experiments done in triplicates

The cytotoxic effects of the peptides toward differentiated and undifferentiated 3T3-L1 cells were also investigated. It was observed that IPI, STYV and STY was not cytotoxic compared with the untreated controls (Fig. 3). However, at 100 µM, SEPA showed significant (P<0.05) cytotoxic effects to both differentiated and undifferentiated cells while 100 µM SVPA

displayed significant (P< 0.05) only against undifferentiated 3T3-L1 cells. Interestingly, 50 and 100 μM, GSH was cytotoxic in undifferentiated but not differentiated 3T3-L1 cells.

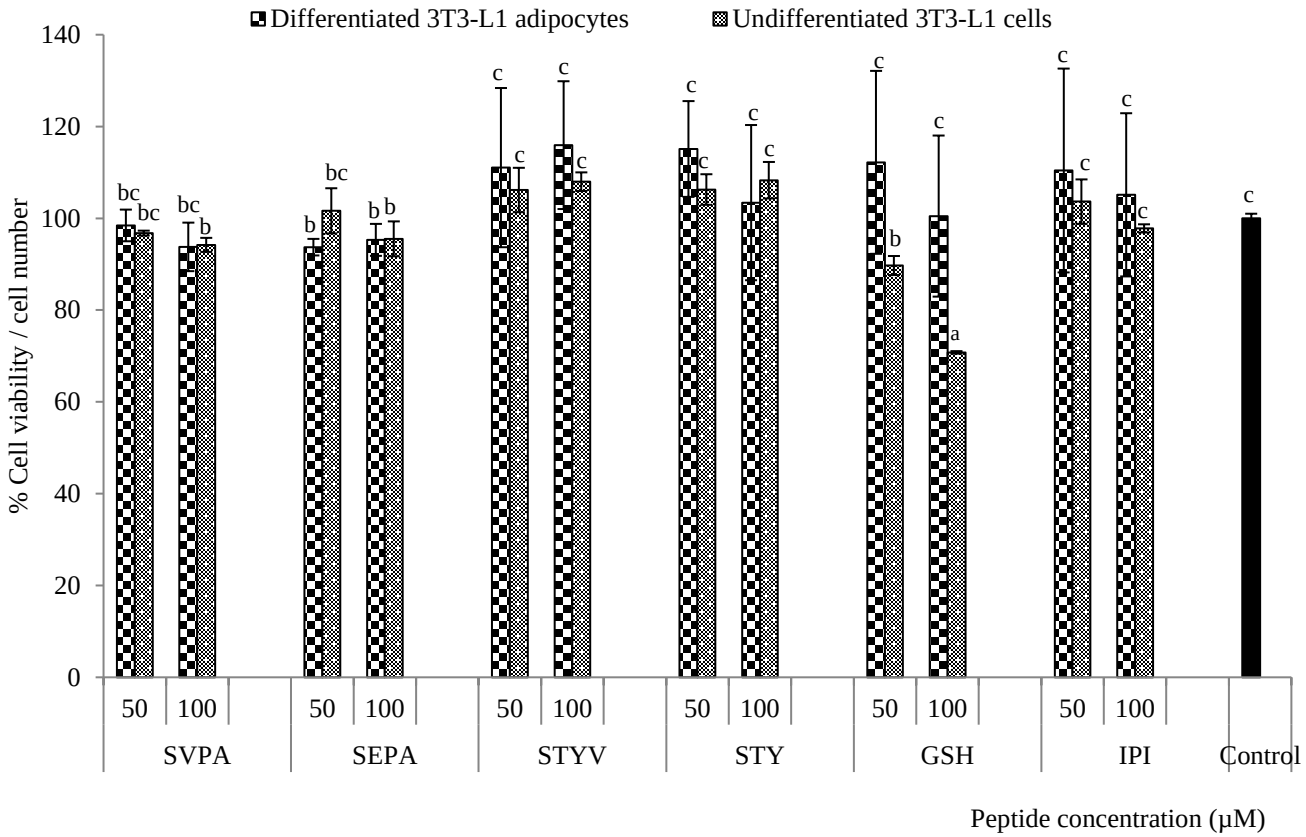

Fig. 3 Cytotoxicity profile of SVPA, SEPA, STYV and STY on differentiated 3T3-L1 adipocytes and undifferentiated 3T3-L1 cells. Cell viability in the presence of the peptides was expressed as a percentage of the vehicle control. Data are expressed as mean ± SD of two independent experiments done in triplicates. [a-b]Values with different subscript letters over the bars are significantly different from each other (Tukey's-HSD multiple range post hoc test, P < 0.05).

To understand the effects of the peptides on adipocyte differentiation process and lipid accumulation, two experimental strategies were employed. Three days post-confluent, the 3T3-L1 cell cultures were induced to differentiate into adipocytes with the differentiation medium containing 50 and 100 μM of the peptides while control cultures were maintained with the normal differentiation medium. At both 50 and 100 μM, SVPA, STYV and STY significantly (P<0.05) decreased the lipid content of the differentiated 3T3-L1 adipocytes while the reduction in the lipid content for SEPA and GSH were not significant (P>0.05) (Fig. 4A). Although the data was significant (P<0.05), the reduction in lipid content caused by the SVPA, STYV and

STY was approximately in the range of 5 – 14%. The Oil Red O staining revealed (Fig. 5A) dense monolayers, with slightly spindle shaped cells that stained red. Adipocytes exposed to SVPA and SEPA, were more rounded and the distribution more sparse compared with the control and cultures exposed to STYV, STY, GSH and IPI. This morphology is usually associated with toxicity and may reflect the decrease in cell viability observed in Fig. 3, for differentiated adipocytes. In the experiment where the adipocytes were exposed to a 50 and 100 μM peptide for 24 h after the differentiation, the quantitative analysis of the lipid content showed that STY (50 μM), GSH (100 μM), and IPI significantly (P<0.05) reduced the lipid content in the 3T3-L1 differentiated adipocytes (Fig. 4B) and these reductions were, approximately, in the range of 6-9%. Evaluation of Oil Red O staining (Fig. 5B) revealed cellular distribution and staining similar to Figure 5A. Reduced density observed for SVPA and SEPA indicates that these peptides may be more cytotoxic compared to the other peptides, although the effects are small, and may not be biologically significant. Moreover, only STY, GSH and IPI showed a slight reduction in intracytoplasmic lipid accumulation when the 3T3-L1 adipocytes were exposed to the peptides for 24 hours after the differentiation process was completed at day 14 (Fig. 5B).

The ability of the peptides to scavenge MG to form AGEs was determined (Fig. 6). All the peptides including diprotin A showed a concentration-dependent scavenging ability. Although the results were not significantly different (P>0.05), SVPA and SEPA had a higher scavenging potential of MG to form AGEs than STYV while STY had the least MG scavenging potential. For STY, the AGEs formed was significantly (P<0.05) lower than the amount of AGEs formed with SVPA and SEPA at all the concentrations (Fig. 6) and was comparable with GSH.

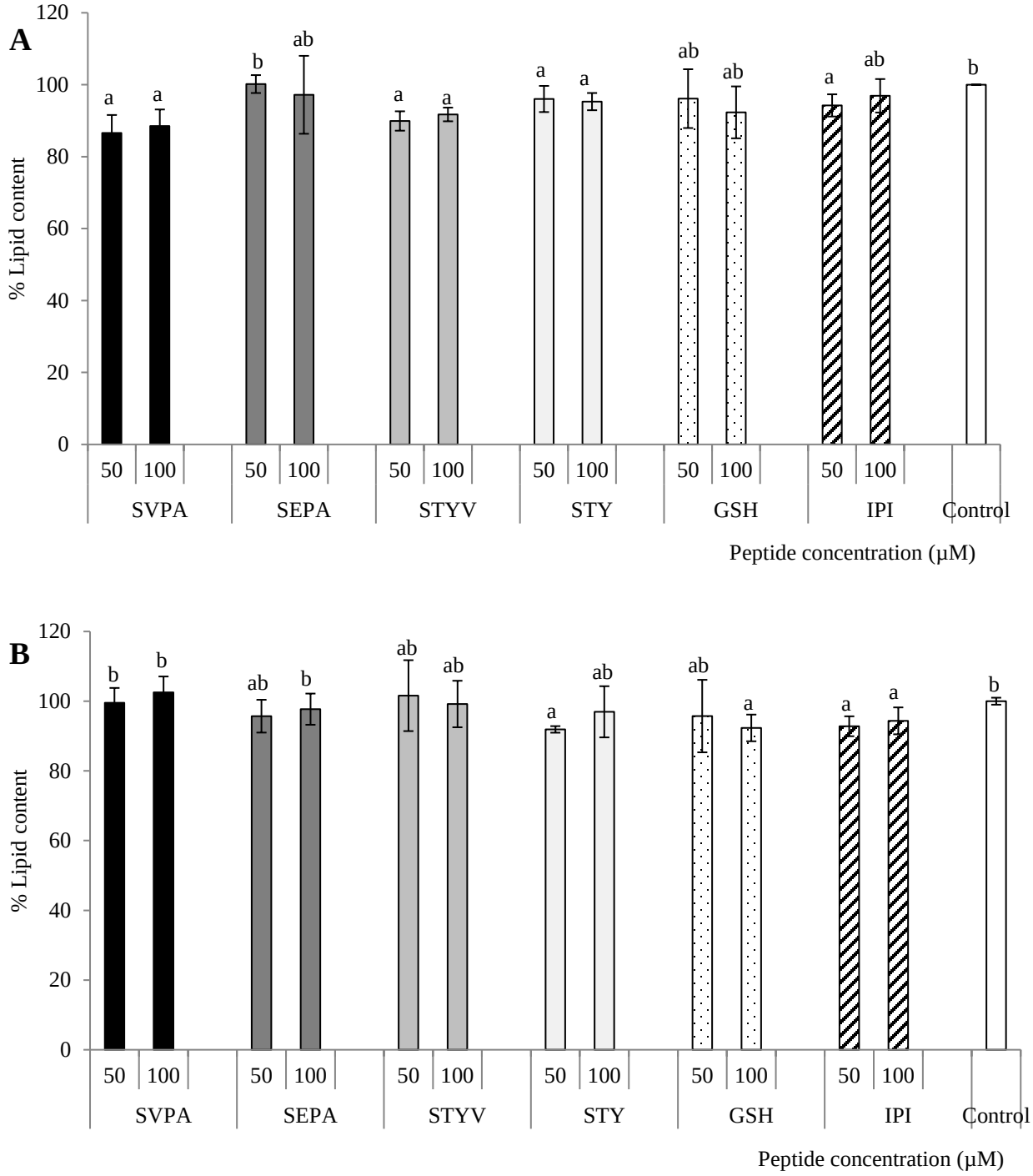

Fig. 4 Quantitative analysis of lipid accumulation in Oil Red O stained 3T3-L1 differentiated adipocytes in the presence of SVPA, SEPA, STYV and STY during (**A**) and after (**B**) the differentiation process. Lipid accumulation in the presence of the peptides was expressed as a percentage of the vehicle control. Data are expressed as mean ± SD of two independent experiments done in triplicates. [a-b]Values with different subscript letters over the bars are significantly different from each other (Tukey's-HSD multiple range post hoc test, $P < 0.05$).

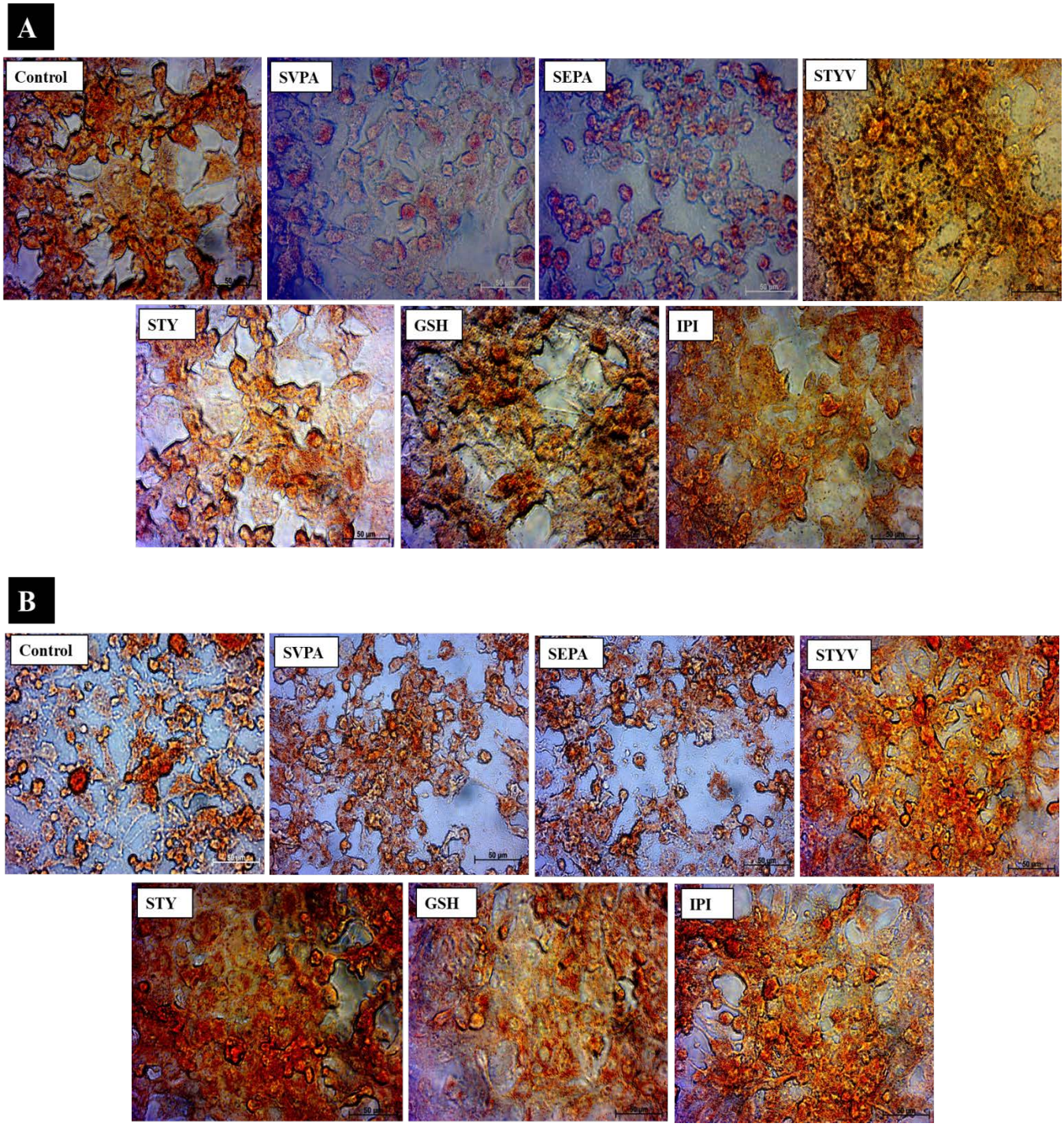

Fig. 5 Representative micrographs showing the effects of SVPA, SEPA, STYV and STY (at 100 µM) on lipid accumulation of 3T3-L1 adipocytes exposed to the peptides during (**A**) and after (**B**) the differentiation events assessed by Oil Red O staining. The cells were photographed at magnification x40.

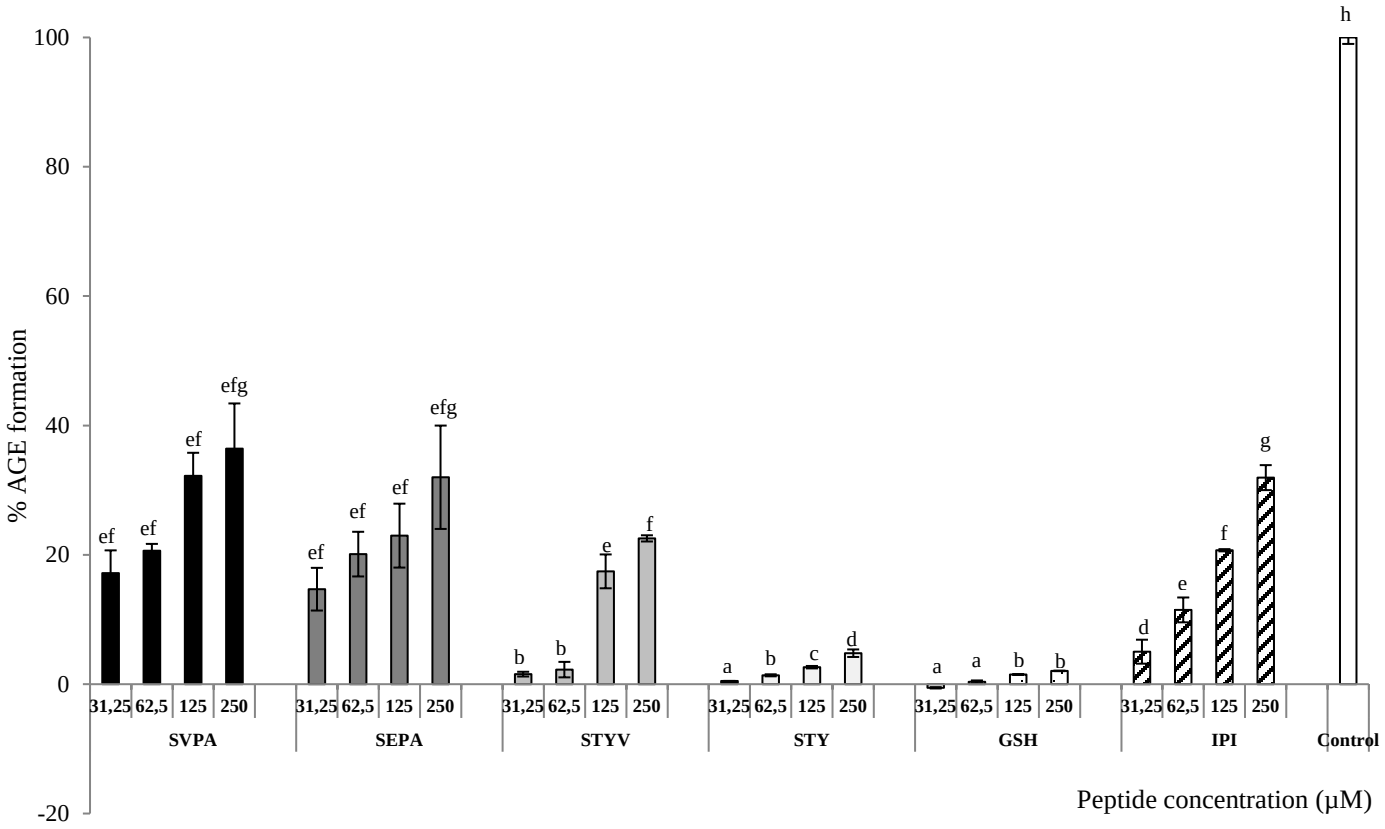

Fig. 6 Interaction of different concentrations of SVPA, SEPA, STYV, STY, GSH and IPI with MGO to form AGEs. Data are expressed as mean ± SD of two independent experiments done in triplicates. [a-h]Values with different subscript letters over the bars are significantly different from each other (Tukey's-HSD multiple range post hoc test, $P < 0.05$)

The oxygen radical quenching capacity of the peptides was determined with the ORAC assay. The scavenging activity of STYV was significantly higher ($P<0.05$) than SVPA and SEPA at all the tested concentrations (Fig. 7). In comparison to STY, STYV also showed a higher, though insignificant ($P >0.05$), oxygen radical scavenging activity. Interestingly, at all the concentrations (5 – 50 µM), STYV and STY also had a significantly ($P< 0.05$) higher radical scavenging activity than the positive controls, GSH and IPI (Fig. 7). For NO scavenging activity, STY showed a significantly ($p < 0.05$) higher activity than SVPA and SEPA while the data were comparable to STYV except at 12.5 and 100 µM (Fig. 8). GSH also showed similar NO scavenging activity to STY at most of the concentrations while IPI was comparable to STY at lower concentrations (12.5 - 25 µM) only (Fig. 8).

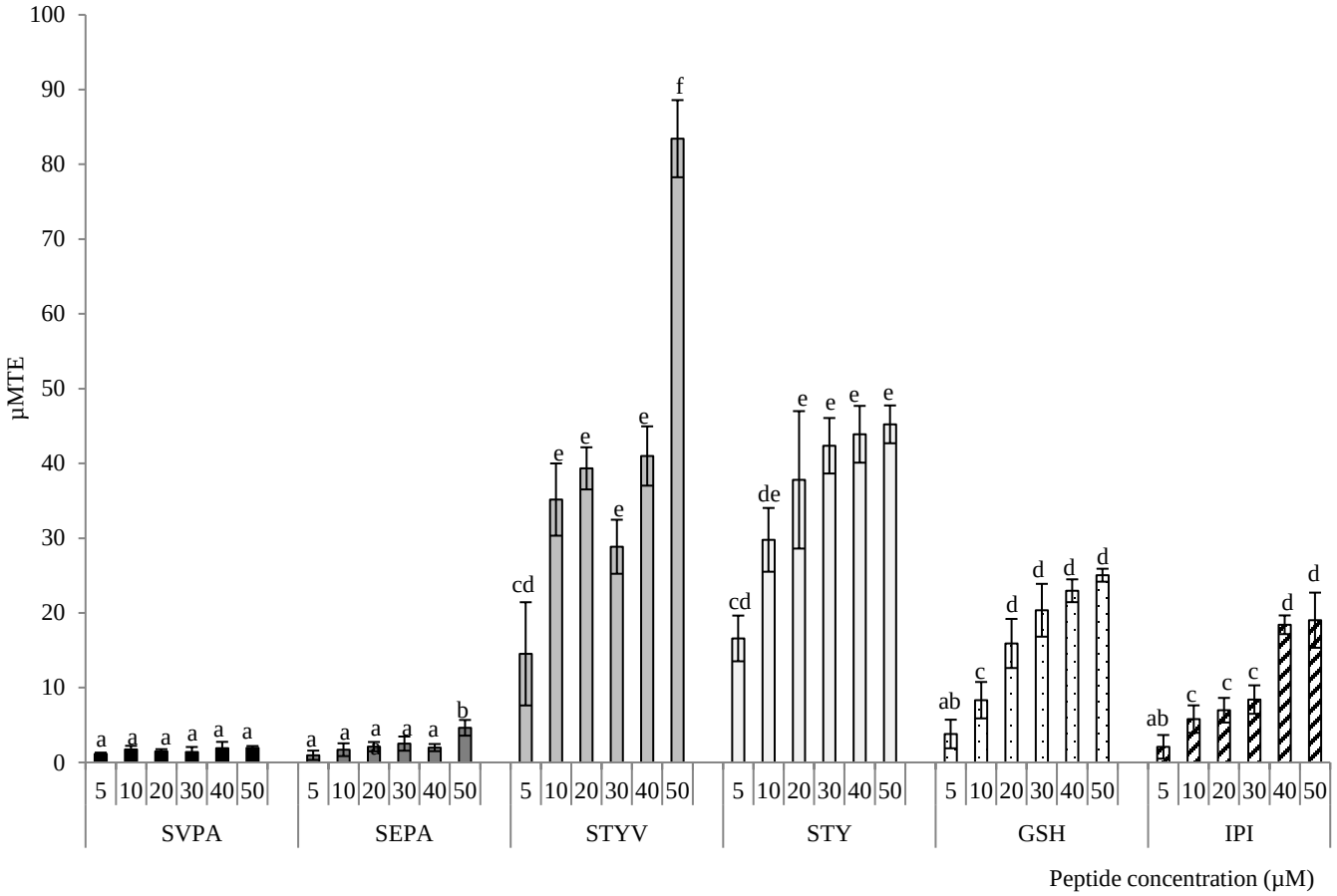

Fig. 7 Oxygen radical absorbance capacity (ORAC) based antioxidant activity of different concentrations of SVPA, SEPA, STYV, STY, GSH and IPI. Data are expressed as mean ± SD of two independent experiments done in triplicates. [a-f]Values with different subscript letters over the bars for a given concentration are significantly different from each other (Tukey's-HSD multiple range post hoc test, $P < 0.05$)

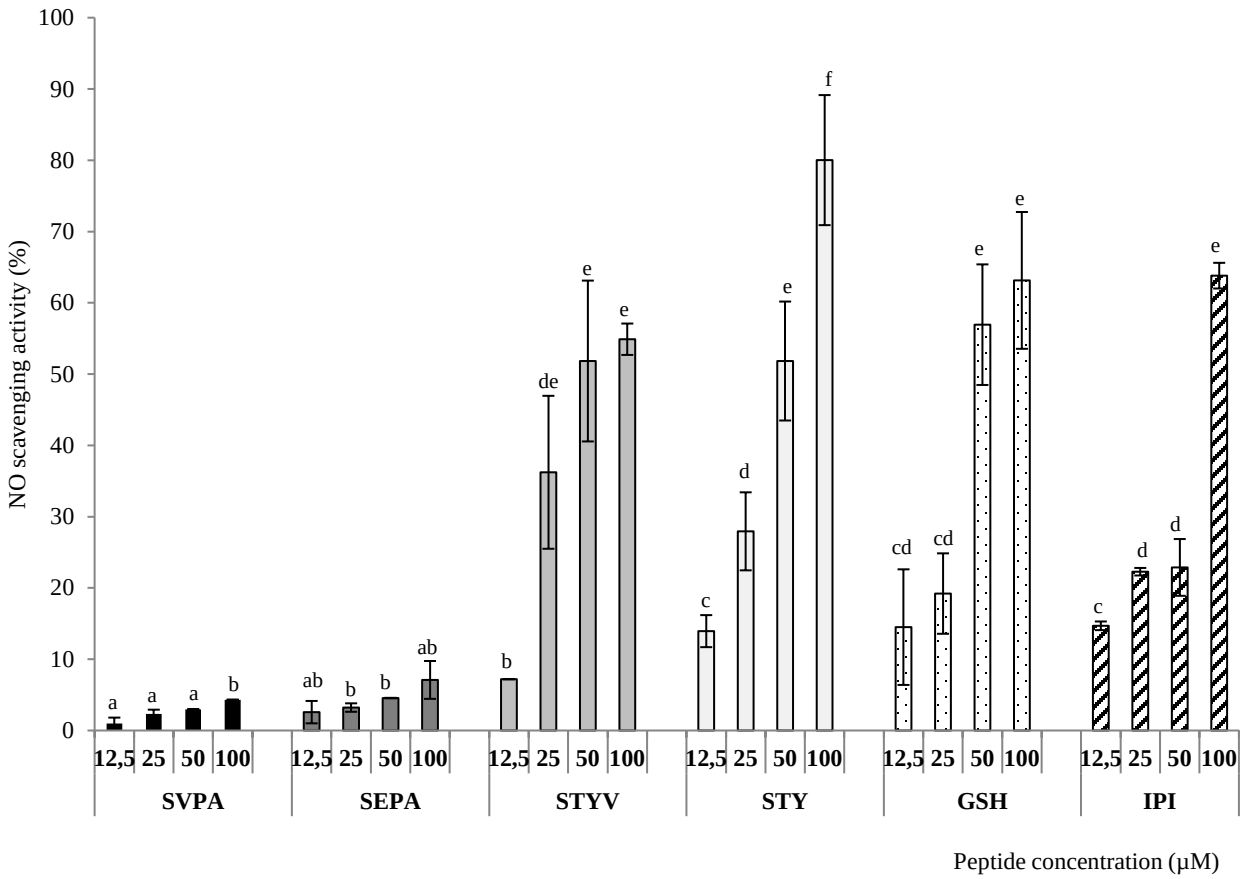

Fig. 8 Nitric oxide (NO) scavenging activity of SVPA, SEPA, STYV, STY, GSH and IPI. The amount of NO scavenged in the presence of the peptides was expressed as a percentage of a control containing all reagents except the peptides. Data are expressed as mean ± SD of two independent experiments done in triplicates. $^{a-f}$Values with different subscript letters over the bars for a given concentration are significantly different from each other (Tukey's-HSD multiple range post hoc test, $P < 0.05$)

Discussion

In T2DM, the identification of multiple therapeutic targets has led to the development of distinct classes of antidiabetic drugs that act on specific targets (Tiwari et al. 2014). Therefore, antidiabetic agents with more than one therapeutic target would be beneficial to the diabetic patients. In this study, we report the effects of four α-glucosidase inhibitory peptides (SVPA, SEPA, STYV and STY) on DPP-IV activity, 3T3-L1 cell viability, lipid accumulation in 3T3-L1 differentiated adipocytes, as well as the ability of these peptides to scavenge MG, ROS and NO with the aim to increase pharmaceutical potential of the peptides as multifunctional agents.

Unlike di- and tripeptides, tetrapeptides have not been extensively studied as potential DPP-IV inhibitors (Nongonierma et al. 2013; Nongonierma et al. 2014; Lafarga et al. 2014) and

it was interesting to observe that the tetrapeptides in the present study had lower binding free energy against the human DPP-IV than the tripeptide (STY). In fact, the binding free energy of the SVPA, SEPA and STYV is lower than the binding free energy of most of the previously docked di-and tripeptides using the same software (Nongonierma et al. 2013; Nongonierma et al. 2014) demonstrating their possible DPP-IV inhibitory potential. Moreover, the observed higher binding affinities of SVPA and SEPA than STYV could be linked to the presence of proline residue at the penultimate position which is known feature of DPP-IV inhibitory peptides (Nongonierma and FitzGerald 2016). However, STYV had more hydrogen bond interactions with the active site residues which suggest a competitive-like type of interaction for STYV and non-competitive type for the other peptides. It appears that the S1 on the peptide might be an important residue for binding at the active site of the enzyme. This is because the 2/3 of the interactions of STYV were mediated through the S1 residue while 0/6 interactions of SEPA and only 1/3 interactions of STY, were mediated through the same residue.

In a previous study, we reported the α-glucosidase inhibitory activity of SVPA and SEPA (Ibrahim et al. 2018b) and therefore, it was necessary to initially also validate the α-glucosidase inhibitory activity of STYV in our laboratory alongside the predicted digested fragment, STY, before subjecting all the peptides to the DPP-IV inhibition assay. STYV had the best α-glucosidase inhibitory activity compared to the other peptides which supports the previous observation where STYV was found to have the best activity among the 43 fully sequenced α-glucosidase inhibitory peptides reported in the literature (Ibrahim et al. 2018a). However, the IC_{50} value of 0.35 ± 0.09 mM observed in the present study was higher than the reported 0.012 μM for the same peptide (Singh and Kaur 2015; Ibrahim et al. 2018a) under the same assay protocols. This clearly demonstrates the need to compare data across laboratories before a definite statement is made about the potency of α-glucosidase inhibitory peptides. For the *in vitro* DPP-IV inhibition, SEPA had the best activity compared to the other peptides except diprotin A and the data did not agree with the molecular docking analysis where SVPA showed the best binding affinity. In spite of this observation, it was noteworthy that the peptides with proline at the penultimate position had the better DPP-IV inhibitory activity which supports a previous study (Nongonierma and FitzGerald 2016). This might further suggest that SEPA could have the ability to inhibit DPP-IV to increase the half-life of glucose-dependent insulinotropic

polypeptide and glucagon-like peptide 1 and consequently, decrease blood glucose levels (Lacroix and Li-Chan 2016). Further enzyme kinetic analysis revealed that SEPA and SVPA could inhibit DPP-IV using both competitive and non-competitive patterns whilst STYV and STY are uncompetitive inhibitors. This means that SEPA and SVPA could bind at the active site or at a site distant from the active site to eventually prevent the binding of the DPP-IV substrates at the active site while STYV and STY could only interact with the enzyme-substrate complex. In fact, the observed modes of DPP-IV inhibition of the peptides are different from the competitive inhibition known to be exhibited by diprotin A (IPI) which is a standard peptidic inhibitor for the enzyme. The competitive mode of DPP-IV inhibition by diprotin A has been linked to the penultimate proline residue in the peptide but with respect to SEPA and SVPA, the present findings tend to suggest that, in addition to the penultimate proline residue, the number and nature of amino acid residues in a peptide might play a role in the mode of DPP-IV inhibition.

Adipocytes are the primary cells in adipose tissue and play important roles in metabolic systems and insulin action which make them targets for another class of antidiabetics, the glitazones (Zilleßen et al. 2016). Adipocyte dysfunction causes lipodystrophy and lipid accumulation which eventually contribute to the development of macrovascular complications of T2DM. In adipocytes, a beneficial therapeutic molecule can either alter lipid metabolism or have selective cytotoxicity (Semaan et al. 2018). The peptides SVPA, STYV and STY retarded lipid accumulation while cytotoxicity was observed for SEPA when added after or during differentiation. Interestingly, GSH was cytotoxic to undifferentiated but not differentiated adipocytes. Likewise, SVPA showed some degree of cytotoxicity in undifferentiated adipocytes. ROS are important cell signaling molecules and accelerate the expansion as well as the differentiation of 3T3-L1 cells (Lee et al. 2009) where the antioxidants genistein and resveratrol arrest the expansion of the cell population and reduce adipocyte differentiation. Caffeic acid methyl esters (Eid et al. 2017) were also found to inhibit lipid accumulation. Diprotin A, IPI favours lipolysis in differentiated adipocytes by triggering the activity of downstream lipases which have been implicated in the lipolysis process of adipocytes (Saito et al. 2007). In the present study, IPI was identified as a peptide with antioxidant activity, which can reduce ROS levels with the potential to inhibit mitotic expansion and 3T3-L1 differentiation. However, no

change in the 3T3-L1 cell viability was observed indicating that IPI, may affect lipolysis rather than differentiation. The effect of IPI, GSH and STY, on differentiated 3T3 L1 adipocytes indicates that lipolysis is favoured. In contrast, SEPA does not scavenge ROS and did not affect lipid accumulation but was cytotoxic in differentiated 3T3-L1 adipocytes at both 50 and 100 μM indicating selective cytotoxicity which has been identified by Semaan et al. (2018) as a possible mechanism. SVPA, STYV and STY reduced lipid levels by 5-14% with SVPA being a poor and STYV and STY being strong antioxidant peptides. The effect of SVPA may be related to the DPP-IV inhibitory activity of the peptide as DPP-IV knockdown has been reported to contribute to adipocyte maturation by mimicking growth factor withdrawal during the early phase of adipocyte differentiation (Zilleßen et al. 2016). Based on the foregoing, it could be inferred that the presence of a proline residue at a penultimate position of a peptide might not be a crucial requirement for preventing lipid accumulation in differentiated adipocytes while amino acids with hydroxyl groups might be relevant in this regard.

MG is a highly reactive dicarbonyl aldehyde whose elevated levels has been linked with insulin resistance, pancreatic β-cell dysfunction as well as micro- and macrovascular complications associated with T2DM (Matafome et al. 2017). Therefore, MG scavenging is receiving attention as a therapeutic strategy which has led to the development of experimental drugs such as edaravone and alagebrium, both with limited effects (Dhar et al. 2010; Li et al. 2013). Interestingly, the peptides, especially, SVPA, SEPA and STYV (125 - 250 μM) have shown good MG scavenging activity suggesting that these peptides may impede the detrimental consequences of elevated MG levels under diabetic conditions. MG-dependent inhibition of insulin receptor pathway has been shown to retard the formation of lipid droplets in 3T3-L1 adipocytes (Rodrigues et al. 2017). Thus, inhibition of lipid accumulation by SVPA may be due to this effect. Moreover, STYV, but not STY, scavenged MG indicating that the valine, in STYV, contributes to the MG scavenging effect of the peptide. Both SVPA, SEPA and STY have N-terminal serine residues but only STY had no MG scavenging activity suggesting that the C-terminal alanine and/or proline residues may contribute to MG scavenging activity. This is an impressive finding because no MG scavenging activity has been previously ascribed to hydrophobic amino acids. IPI, with two hydrophobic amino acids also effectively scavenges MG which further agrees with the earlier assertion. However, in larger proteins, these amino acids

may not be the MG targets as these amino acids are usually buried in the hydrophobic core of proteins.

Endothelial dysfunction is a feature of T2DM and the associated risk for the development of cardiovascular disease. Endothelial nitric oxide synthetase (eNOS) produces vasoactive NO and the uncoupling of the eNOS results in increased oxidative stress where the uncoupled eNOS forms superoxide anion rather than NO. T2DM is associated with the activation of inducible NOS (iNOS) and increased NO levels that activate inflammatory pathways (Varga et al. 2015) which consequently make profound contribution to the induction of oxidative stress, a phenomenon known to be an important mechanism for the disease pathogenesis and the associated complications. Hence, antioxidant activity is considered as an important feature of potential antidiabetic agents. Both STYV and STY are strong scavengers of ROS and NO, while in contrast SEPA and SVPA are weak scavengers. The ROS scavenging activity of the STYV and STY was greater than the ROS scavenging activity of GSH and IPI while the NO scavenging activity was comparable to GSH and slightly greater than IPI. Hence, the strong ROS and NO scavenging activities of STYV and STY could be attributed to the phenolic side chain of tyrosine contained in these peptides because phenolic group is highly recognised for mediating antioxidant activity (Ibrahim et al. 2014). Therefore, these peptides will help prevent endothelial dysfunction and inflammation by modulating both ROS and NO levels and thereby reducing the risk of T2DM associated pathology.

In conclusion, the predominant effect of STYV and STY is the inhibition of α-glucosidase and lipid accumulation in differentiated 3T3-L1 adipocytes. The additional scavenging of MG, ROS and NO by STYV; and the ROS and NO scavenging activity of STY, identifies both as multifunctional peptides that can prevent several pathologies associated with T2DM. In contrast, SEPA and SVPA are better DPP-IV inhibitors and reduce the lipid content of differentiated 3T3-L1 adipocytes but can only scavenge MG. The different modes of action make these peptides interesting candidates for combination studies, for possible synergistic interactions. Overall, the peptides demonstrated interesting multifunctional antidiabetic activities but the DPP-IV inhibitory activities could be considered to be low and therefore, our future studies will focus on different biochemical strategies to increase the potency and therapeutic viability.

Acknowledgement

We acknowledge the National Research Foundation of South Africa and the University of Pretoria for financial support. The first author also acknowledges the University of Pretoria for the award of a postdoctoral fellowship position in Biochemistry and Ahmadu Bello University, Zaria, Nigeria for the award of a study fellowship.

Compliance with Ethical Standards

Funding: The study was funded by the National Research Foundation of South Africa (Grant Number 91052)

Disclosure of Potential Conflicts of interest: Mohammed Auwal Ibrahim, June Serem, Megan Bester, Albert Neitz and Anabella Gaspar have declared that they have no conflict of interest.

Research involving Human Participants and/or Animals: This article does not contain any studies with human participants or animals performed by any of the authors.

References

Agyei D, Tsopmo A, Udenigwe CC (2018) Bioinformatics and peptidomics approaches to the discovery and analysis of food-derived bioactive peptides. Anal Bioanal Chem 410:3463-3472. https://doi.org/10.1007/s00216-018-0974-1

Byun HG, Lee JK, Park HG, Jeon JK, Kim SK (2009) Antioxidant peptides isolated from the marine rotifer, *Brachionus rotundiformis*. Process Biochem 44:842-846. https ://doi.org/10.1016/j.procb io.2009.04.003

Cao MM, Lu X, Liu GD, Su Y, Li YB, Zhou J (2018) Resveratrol attenuates type 2 diabetes mellitus by mediating mitochondrial biogenesis and lipid metabolism via Sirtuin type 1. Exp Ther Med 15:576-584. https://doi.org/10.3892/etm.2017.5400

De Fronzo RA, Triplitt CL, Abdul-Ghani M, Cersosimo E (2014) Novel agents for the treatment of type 2 diabetes. Diabetes Spectrum 27:100-112. https://doi.org/10.2337/diaspect.27.2.100

Dhar A, Desai KM, Wu L (2010) Alagebrium attenuates acute methylglyoxal-induced glucose intolerance in Sprague-Dawley rats. Br J Pharmacol 159:166–175. https://doi.org/10.1111/j.1476-5381.2009.00469.x

Hasan MM, Ahmed QU, Soad SZM, Latip J, Taher M, Syafiq TMF, Sarian MN, Alhassan AM, Zakaria ZA (2017) Flavonoids from *Tetracera indica* Merr. induce adipogenesis and exert glucose uptake activities in 3T3-L1 adipocyte cells. BMC Complement Altern Med 17:431. https://doi.org/10.1186/s12906-017-1929-3

Eid HM, Thong F, Nachar A, Pierre SH (2017) Caffeic acid methyl and ethyl esters exert potential antidiabetic effects on glucose and lipid metabolism in cultured murine insulin-sensitive cells through mechanisms implicating activation of AMPK. Pharm Biol 55:2026-2034. https://doi.org/10.1080/13880209.2017.1345952

Giacco F, Brownlee M (2010) Oxidative stress and diabetic complications. Circ Res 107:1058-1070. https://doi.org/10.1161/CIRCRESAHA.110.223545

Giustarini D, Rossi R, Milzani A, Dalle-Donne I (2008) Nitrite and nitrate measurement by Griess reagent in human plasma: evaluation of interferences and standardization. Methods Enzymol 440:361–380. https://doi.org/10.1016/S0076-6879(07)00823-3

Guariguata L, Whiting DR, Hambleton I, Beagley J, Linnenkamp U, Shaw JE (2014) Global estimates of diabetes prevalence for 2013 and projections for 2035. Diabetes Res Clin Pract 103:137-149. https://doi.org/10.1016/j.diabres.2013.11.002

Hadi HAR, Suwaidi JA (2007) Endothelial dysfunction in diabetes mellitus. Vasc Health Risk Manag 3:853-876.

Ibrahim MA, Bester MJ, Neitz AWH, Gaspar ARM (2018a) Structural properties of bioactive peptides with α-glucosidase inhibitory activity. Chem Biol Drug Des. 91:370 -379. https://doi.org/10.1111/cbdd.13105

Ibrahim M. A., Bester M.J., Neitz A.W.H. and Gaspar A. R. M. (2018b). Rational *in silico* design of α-glucosidase inhibitory peptides and *in vitro* evaluation of promising candidates. Biomed Pharm 107:234 -242. https://doi.org/10.1016/j.biopha.2018.07.163

Ibrahim MA, Koorbanally N, Islam MS (2014) Anti-oxidative activity and inhibition of key enzymes linked to type 2 diabetes (α-glucosidase and α-amylase) by *Khaya senegalensis*. Acta Pharm 64:311-324. https://doi.org/10.2478/acph-2014-0025

Inzucchi SE, Bergenstal RM, Buse JB, Diamant M, Ferrannini E, Nauck M, Peters AL, Tsapas A, Wender R, Matthews DR (2015) Management of hyperglycaemia in type 2 diabetes, 2015: a patient-centred approach. Update to a position statement of the American Diabetes Association and the European Association for the Study of Diabetes. Diabetologia 58:429-442. https://doi.org/10.2337/dc14-2441

Konrad B, Dabrowski A, Szoltysik M, Marta P, Aleksandra Z, Jozefa C (2014) The evaluation of dipeptidyl peptidase (DPP)-IV, α-glucosidase and angiotensin converting enzyme (ACE) inhibitory activities of whey proteins hydrolysed with serine protease isolated from Asian

pumpkin *(Cucurbita ficifolia*). Int J Pept Res Ther 20:483-491. https://doi.org/10.1007/s10989-014-9413-0

Korhonen H, Pihlanto A (2007) Food-derived bioactive peptides-opportunities for designing future foods. Curr Pharm Des 9:1297-1308. https://doi.org/10.2174/1381612033454892

Lacroix IM, Li-chan EC (2016) Food-derived dipeptidyl-peptidase IV inhibitors as potential approach for glycemic regulation–Current knowledge and future research considerations. Trends Food Sci Technol 54:1-16. https://doi.org/10.1016/j.tifs.2016.05.008

Lafarga T, Connor PO, Hayes M (2014) Identification of novel dipeptidyl peptidase-IV and angiotensin-I-converting enzyme inhibitory peptides from meat proteins using *in silico* analysis. Peptides 59:53-62. https://doi.org/10.1016/j.peptides.2014.07.005

Lee H, Lee YJ, Choi H, Ko EH, Kim J (2009) Reactive oxygen species facilitate adipocyte differentiation by accelerating mitotic clonal expansion. J Biol Chem 280:10601–10609. https://doi.org/10.1074/jbc.M808742200

Li Q, Zhang C, Chen H, Xue J, Guo X, Liang M, Chen M (2018) BioPepDB: an integrated data platform for food-derived bioactive peptides. Int J Food Sci Nutr 69:963-968 https://doi.org/10.1080/09637486.2018.1446916

Li W, Xu H, Hu Y, He P, Ni Z, Xu H, Zhang Z, Dai H (2013) Edaravone protected human brain microvascular endothelial cells from methylglyoxal-induced injury by inhibiting AGEs/RAGE/oxidative stress. PLoSOne 8:e76025. https://doi.org/10.1371/journal.pone.0076025

Matafome P, Rodrigues T, Sena C, Seiça R (2017) Methylglyoxal in metabolic disorders: Facts, myths, and promises. Med Res Rev 37:368-403. https://doi.org/10.1002/med.21410

Mojica L, de Majia MG (2016) Optimization of enzymatic production of anti-diabetic peptides from black bean (*Phaseolus vulgaris* L.) proteins, their characterization and biological potential. Food Funct 7:713-727. https://doi.org/10.1039/C5FO01204J

Nongonierma AB, FitzGerald RJ (2016) Structure activity relationship modelling of milk protein-derived peptides with dipeptidyl peptidase IV (DPP-IV) inhibitory activity. Peptides 79: 1-7. https://doi.org/10.1016/j.peptides.2016.03.005

Nongonierma AB, Mooney C, Shields DC, FitzGerald RJ (2013) Inhibition of dipeptidylpeptidase IV and xanthine oxidase by amino acids and dipeptides. Food Chem 141:644–53. https://doi.org/10.1016/j.foodchem.2013.02.115

Nongonierma AB, Mooney C, Shields DC, FitzGerald RJ (2014) *In silico* approaches to predict the potential of milk protein-derived peptides as dipeptidyl peptidase IV (DPP-IV) inhibitors. Peptides 54:43-51. https://doi.org/10.1016/j.peptides.2014.04.018

Ou B, Huang D, Hampsch-Woodill M, Flanagan JA, Deemer EK (2002) Analysis of antioxidant activities of common vegetables employing oxygen radical absorbance capacity (ORAC) and ferric reducing antioxidant power (FRAP) assays: a comparative study. J Agric Food Chem 50: 3122–3128. https://doi.org/10.1021/jf0116606

Park YW, Nam MS (2015) Bioactive peptides in milk and dairy products: a review. Korean J Food Sci Animal Res 35:831-840. https://doi.org/10.5851/kosfa.2015.35.6.831

Pettersen EF, Goddard TD, Huang CC, Couch GS, Greenblatt DM, Meng EC, Ferrin TE (2004) UCSF Chimera - a visualization system for exploratory research and analysis. J Comp Chem 25:1605 – 1612. https://doi.org/10.1002/jcc.20084

Rodrigues T, Matafome P, Sereno J, Almeida J, Castelhano J, Gamas L, Neves C, Gonçalves S, Carvalho C, Arslanagic A, Wilcken E (2017) Methylglyoxal-induced glycation changes adipose tissue vascular architecture, flow and expansion, leading to insulin resistance. Sci Rep 7:1698. https://doi.org/10.1038/s41598-017-01730-3

Saito T, Abe D, Sekiya K, (2007). Nobiletin enhances differentiation and lipolysis of 3T3-L1 adipocytes. Biochem Biophys Res Comm 357:371–376. https://doi.org/10.1016/j.bbrc.2007.03.169

Semaan DG, Igoli JO, Young L, Gray AI, Rowan EG, Marrero E (2018) *In vitro* anti-diabetic effect of flavonoids and pheophytins from *Allophylus cominia* Sw. on the glucose uptake assays by HepG2, L6, 3T3-L1 and fat accumulation in 3T3-L1 adipocytes. J Ethnopharmacol 216:8-17. https://doi.org/10.1016/j.jep.2018.01.014

Shai LJ, Masoko P, Mokgotho MP, Magano SP, Mogale AM, Boaduo N, Eloff JN (2010) Yeast alpha glucosidase inhibitory and antioxidant activities of six medicinal plants collected in Phalaborwa, South Africa, South Afr J Bot 76:465–470. https://doi.org/10.1016/j.sajb.2010.03.002

Singh B, Kaur A (2015) Antidiabetic potential of a peptide isolated from an endophytic *Aspergillus awamori*. J App Microbiol 120:301-311. https://doi.org/10.1111/jam.12998

Siddiqui MA, Rasheed S, Saquib Q, Al-Khedhairy AA, Al-Said MS, Musarrat J, Choudhary MI (2016) *In vitro* dual inhibition of protein glycation, and oxidation by some Arabian plants. BMC Complement Altern Med 16:276. https://doi.org/10.1186/s12906- 016-1225-7

Tiwari N, Thakur AK, Kumar V, Dey A, Kumar V (2014) Therapeutic targets for diabetes mellitus: an update. Clin Pharmacol Biopharm 3:117. https://doi.org/10.4172/2167-065X.1000117

Trott O, Olson AJ (2010) AutoDock Vina: improving the speed and accuracy of docking with a new scoring function, efficient optimization and multithreading. J Comp Chem 31:455–461. https://doi.org/10.1002/jcc.21334

Udenigwe CC (2014) Bioinformatics approaches, prospects and challenges of food bioactive peptide research. Trends Food Sci Technol 36:137–143. https://doi.org/10.1016/j.tifs.2014.02.004

Usmani, S.S., Bedi, G., Samuel, J.S., Singh, S., Kalra, S., Kumar, P., Ahuja, A.A., Sharma, M., Gautam, A. and Raghava, G.P., (2017). THPdb: Database of FDA-approved peptide and protein therapeutics. *PloS One*, *12*(7), p.e0181748. https://doi.org/10.1371/journal.pone.0181748

Varga ZV, Giricz Z, Liaudet L, Haskó G, Ferdinandy P, Pacher P (2015) Interplay of oxidative, nitrosative/nitrative stress, inflammation, cell death and autophagy in diabetic cardiomyopathy. Biochim Biophys Acta 1852:232-242. https://doi.org/10.1016/j.bbadis.2014.06.030

Vulesevic B, McNeill B, Giacco F, Maeda K, Blackburn NJ, Brownlee M, Milne RW, Suuronen EJ (2016) Methylglyoxal-induced endothelial cell loss and inflammation contribute to the development of diabetic cardiomyopathy. Diabetes, 65:1699-1713. https://doi.org/10.2337/db15-0568

Wang S, Zeng X, Yang Q, Qiao S (2016) Antimicrobial peptides as potential alternatives to antibiotics in food and animal industry. Int J Mol Sci 17:603. https://doi.org/10.3390/ijms17050603

Wu D, Wang J, Wang H, Ji A, Li Y (2017) Protective roles of bioactive peptides during ischemia-reperfusion injury: From bench to bedside. Life Sci 180:83-92. https://doi.org/10.1016/j.lfs.2017.05.014

Yin CM, Wong JH, Xia J, Ng TB (2013) Studies on anticancer activities of lactoferrin and lactoferricin. Curr Prot Pept Sci 14:492–503. https://doi.org/10.2174/13892037113149990066

Zhang Y, Wang N, Wang W, Wang J, Zhu Z, Li X (2016) Molecular mechanisms of novel peptides from silkworm pupae that inhibit α-glucosidase. Peptides 76:45-50. https://doi.org/10.1016/j.peptides.2015.12.004

Zilleßen P, Celner J, Kretschmann A, Pfeifer A, Racke K, Mayer P (2016).Metabolic role of dipeptidyl peptidase 4 (DPP4) in primary human (pre)adipocytes. Sci Rep 6:23074. https://doi.org/10.1038/srep23074